

**© 2018 IEEE.** Personal use of this material is permitted. Permission from IEEE must be obtained for all other uses, in any current or future media, including reprinting/republishing this material for advertising or promotional purposes, creating new collective works, for resale or redistribution to servers or lists, or reuse of any copyrighted component of this work in other works.

Digital Object Identifier (DOI): 10.1109/IECON.2017.8216731

*IECON 2017 - 43rd Annual Conference of the IEEE Industrial Electronics Society*

**Investigation of load compensation features of smart transformer in medium voltage grid**

Chandan Kumar

Rongwu Zhu

Marco Liserre

**Suggested Citation**

C. Kumar, R. Zhu and M. Liserre, "Investigation of load compensation features of smart transformer in medium voltage grid," *IECON 2017 - 43rd Annual Conference of the IEEE Industrial Electronics Society*, Beijing, 2017, pp. 4260-4265.

# Investigation of Load Compensation Features of Smart Transformer in Medium Voltage Grid

Chandan Kumar, *Member, IEEE*

Department of Electronics and Electrical Engineering  
Indian Institute of Technology Guwahati, India  
chandank@iitg.ernet.in

Rongwu Zhu\*, *Member, IEEE*

Marco Liserre\*\*, *Fellow, IEEE*

Chair of Power Electronics, Faculty of Engineering  
Christian-Albrechts-University of Kiel, Germany  
\*rzh@tf.uni-kiel.de, \*\*ml@tf.uni-kiel.de

**Abstract**—Harmonics and load unbalance create several adverse issues in power distribution system, which are generally mitigated by bulky shunt active power filter (SAPF). This paper explores load compensation features of smart transformer (ST) in a two-feeder city center, where conventional power transformer (CPT) in one feeder is replaced by the ST whereas other feeder is continued to be supplied through the CPT. The ST is controlled not only to supply its own loads connected at the low voltage side, but also to compensate reactive, unbalance and nonlinear loads of the other feeder. This makes total MV grid currents of the combined city center balanced, sinusoidal, and in unity power factor at the point of common coupling (PCC) voltage. Therefore, in addition to providing continuous and reliable support to the ST based loads, the ST eliminates need of bulky SAPF and isolation transformer from the city center which are used for achieving reactive and harmonic current compensation. A switching model of the system is developed in power system computer aided design (PSCAD) software and implemented on a developed experimental prototype to show the capability of the ST.

**Index Terms**—Smart transformer (ST), load compensation, harmonics, power distribution system.

## I. INTRODUCTION

In distribution grid, conventional power transformers (CPTs) are used for achieving voltage transformation and isolation between two voltage levels. The CPTs have limited control feature and designed for unidirectional power flow. However, increase in renewable energy sources (RES), electrical vehicles (EVs), energy storage elements, etc. needs new services as well as restructuring in the electric grid [1]. In this scenario, smart transformer (ST) is an alternative to the CPT in the distribution grid [2], [3]. The ST is a power electronic based transformer having appropriate control and communication features. In addition to basic operational features similar to CPT, the ST also provides benefits like it maintains balanced sinusoidal voltages in low voltage (LV) grid, draws balanced sinusoidal currents from the medium voltage (MV) grid, has dc links for integration of different energy sources, etc [2].

Parallel to research in power electronics for improving efficiency and reliability of ST in the distribution grid, the ST has been explored for possible ancillary services for making its application cost effective [2], [4]. In [5], an ST has been utilized to identify and damp out the grid resonance. A control scheme of ST is presented in [6] to achieve better control and sharing of the power. In [7], an ST has been

proposed for reactive power compensation in the MV grid. A voltage/reactive power control scheme is presented in [8], [9] to minimize the losses in the line and keep the voltages at the feeder within the limits while using several STs and voltage regulators. In [10], a dual microgrid (DMG) operation of ST is proposed.

Load compensation in electric grid is generally achieved with shunt active power filters (SAPFs) [11], [12] and the SAPF supplies currents equal to the harmonic, reactive and unbalanced components of load currents. However, the SAPFs add to the cost of the overall system and also make the system bulky with significant space requirements.

This paper introduces the investigation on the sizing and rating requirements of the ST for load compensation capability as well as its experimental verification in a radial city center consisting of two feeders. In one of the feeders, the CPT is replaced by an ST whereas the other feeder continues to be supplied through the CPT. The ST, while continuously supplying its LV side loads, compensates reactive, unbalance, and harmonic loads of the feeder having CPT. It makes total current of the city center balanced sinusoidal and in phase with the MV point of common coupling (PCC) voltage. This feature of the ST eliminates the requirement of the bulky SAPF from the city center.

The paper is organized as follows. Section II describes the conventional and proposed city center structure. Section III discusses the load compensation capability of ST. Section IV presents detailed explanation of rating requirements of ST, and Section V explains the operation and control of ST. Section VI provides digital simulation results. In Section VII, experimental results are shown. Finally, Section VIII presents the conclusions.

## II. DESCRIPTION OF CONVENTIONAL AND PROPOSED CITY CENTER CONFIGURATIONS

### A. Description of Conventional City Center

Fig. 1(a) shows a single line diagram of a conventional power distribution system consisting of two radial feeders in a city center. Both the feeders use separate CPT, T1 and T2, for supporting the loads. A combination of linear, nonlinear, and unbalanced loads are connected to both the feeders. These

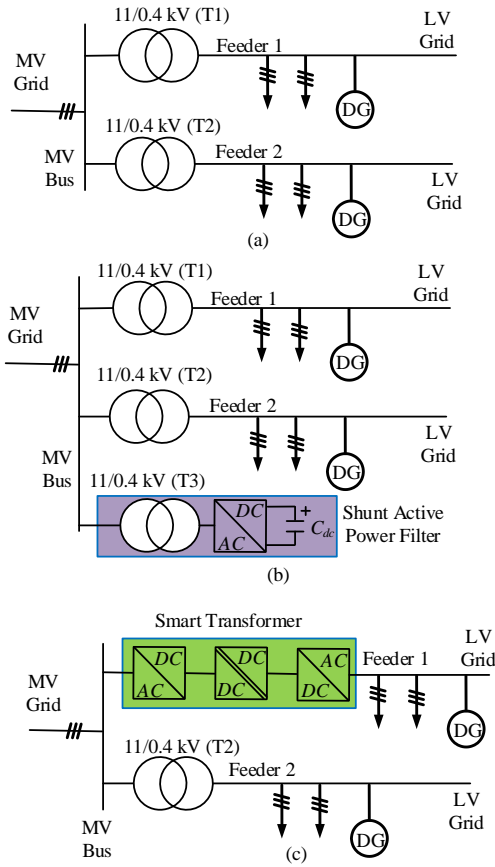


Fig. 1. Single line schematic of two-feeder city center. (a) Conventional system schematic. (b) Conventional system schematic with installation of shunt active power filter for load compensation. (c) Proposed system with one CPT replaced by an ST.

load draw reactive, unbalanced and distorted currents from the MV grid resulting in distorted unbalanced MV grid currents.

Fig. 1(b) shows one of the solution for realizing load compensation features in the city center where a SAPF is installed for compensating the unbalanced, reactive and harmonic loads. The SAPF consists of an ac-dc converter and an isolation transformer T3. Due to space constraints in the city center, installation of SAPF is always a challenging task.

### B. Description of Proposed City Center

In the proposed distribution grid shown in Fig. 1(c), the CPT in one feeder is replaced by the ST whereas another feeder continues to use the CPT. The ST is connected between the MV and LV power distribution system with rating of 11/0.4 kV. With the ST in the feeder 1, the LV side voltage of the ST will be maintained balanced and sinusoidal. Also, the ST will be operated such that the total MV side currents drawn will be balanced and sinusoidal with UPF. With these advantages of the ST, a single ST replaces two CPT and an ac-dc power converter in the two-feeder city center.

This paper uses a three stage ST with two intermediate dc-links. A neutral point clamped (NPC) multilevel converter, as MV converter, is chosen to implement the ac-dc conversion

in the MV side. This converter converts MV ac into MV dc. For converting MV dc to LV dc, a dual active bridge (DAB) converter is used as dc-dc converter. In the LV side, two level VSI is selected to convert the LV dc to LV ac where the loads are connected. The ST supplies power to the loads connected to its LV side and at the same time, offers compensation features to compensate reactive and harmonic components of currents of feeder 2. At this regard, the sizing of the NPC converter depends upon the maximum transferred active power to the LV loads and compensated reactive as well as distorted power of feeder 2.

### III. LOAD COMPENSATION CAPABILITY ANALYSIS OF ST IN CITY CENTER

In the proposed system configuration, the CPT from the feeder 1 is replaced with the ST. The ST operates to support the loads connected to its LV side and additionally, compensates for the reactive and harmonic load of feeder 2. The rating of the ST MV converter is given as follows:

$$S_{mv-con} = \sqrt{3} \frac{V_{mv-dc}}{\sqrt{2}} I_{mv-con} \quad (1)$$

where the terms  $S_{mv-con}$ ,  $I_{mv-con}$ , and  $V_{mv-dc}$  are MV converter apparent power rating, rms current rating of the switch, and capacitor voltage at the MV dc link, respectively. Rearranging the above equation,

$$I_{mv-con} = \sqrt{2} \frac{S_{mv-con}}{\sqrt{3}V_{mv-dc}} \quad (2)$$

Consider  $S_{mv-con}$  as the base power and  $\frac{V_{mv-dc}}{\sqrt{2}}$  as the base voltage. The converter supports real power demand of ST based loads and compensates harmonics as well as reactive current of feeder 2. Let the rms of currents  $I_{act1}$ ,  $I_{reac1}$ , and  $I_{har}$  are fundamental active component, fundamental reactive component, and harmonic component of the MV converter current  $I_{mv-con}$ . Separating the converter current in these three current components, following relation is obtained

$$\sqrt{2} \frac{S_{rec}}{\sqrt{3}V_{dem}} = \sqrt{I_{reac1}^2 + I_{act1}^2 + I_{har}^2} \quad (3)$$

In power electronics interface, power switches are discrete in nature. It generally results in selection of slightly overrated power switches. Taking an overrate factor of 20%, the current rating of MV converter of ST will be 1.2 per unit (p.u.). Converting the above equation in p.u., following relation is obtained

$$I_{reac1} = \sqrt{1.44 - I_{act1}^2 - I_{har}^2} \quad p.u. \quad (4)$$

In above, the currents  $I_{reac1}$  and  $I_{har}$  are currents needed to provide load compensation in MV grid. With the above expression, the reactive current compensation capability curve of ST while supporting loads of LV side of feeder 1 has been drawn and shown in Fig. 2. The capability curve has been drawn for three cases, (a) at 0.1 p.u. harmonic compensation, (b) at 0.2 p.u. harmonic compensation and (c) at 0.3 p.u. harmonic compensation. Case II with 0.2 p.u. harmonic compensation

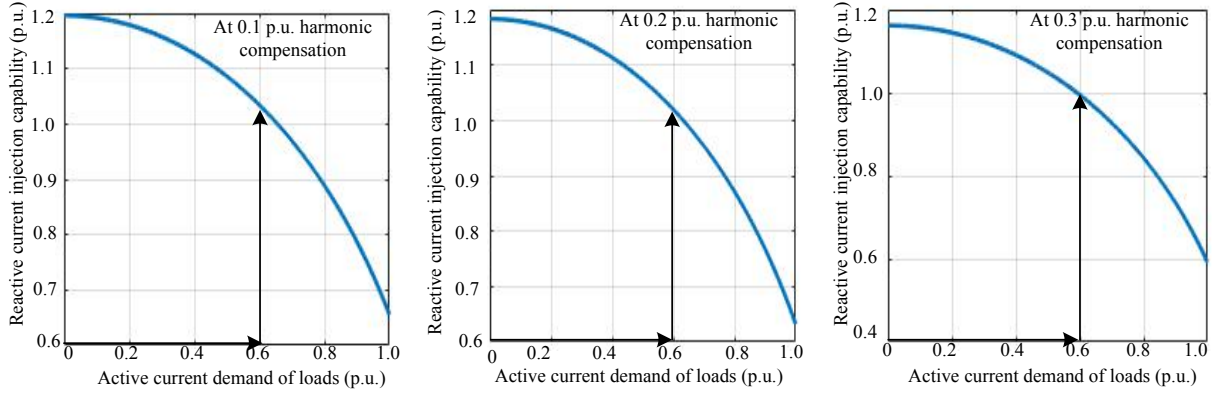


Fig. 2. Reactive current compensation capability curve of ST while supporting loads of LV side of feeder 1. (a) At 0.1 p.u. harmonic compensation. (b) At 0.2 p.u. harmonic compensation. (c) At 0.3 p.u. harmonic compensation.

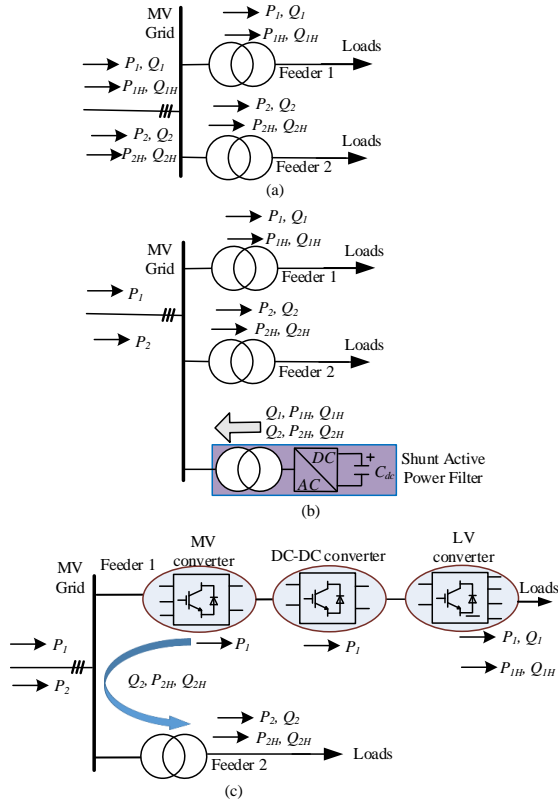


Fig. 3. Power flow diagram in the city center. (a) Conventional distribution grid. (b) SAPF based distribution grid. (c) ST based proposed distribution grid.

can be treated as normal harmonic compensation and case III with 0.3 p.u. harmonic compensation can be treated as worst harmonic scenario in the MV grid. Most of the time of the grid operation, the power requirement of the LV loads remain between 0.4 p.u. to 0.8 p.u. of the total load demand of 1.0 p.u. From the capability curves, it can be noticed that the ST has sufficient capability to compensate the reactive current of the feeder 2. For example, the ST can inject nearly 1 p.u.

of reactive power while supplying to 0.6 p.u. of LV side ac loads. Consequently, the ST has capability to provide the load compensation in MV power system without any burden in the cost and rating requirements of power converters of ST.

#### IV. POWER FLOW DIAGRAM IN CITY CENTER AND SMART TRANSFORMER SIZING

The power flow diagram in the city center for different system configurations is shown in Fig. 3. In conventional system, the load requirements are supplied by the MV grid as shown in Fig. 3(a). Therefore, the transformers T1 and T2 are selected to meet the load demands. When the reactive and harmonic powers are supplied by the SAPF, the corresponding power flow is shown in Fig. 3(b). The transformer T3 and ac-dc converter is rated to support the city center reactive and harmonic loads.

Fig. 3(c) shows power flow in proposed system configuration. The feeder 2 reactive and harmonic currents are supplied by the MV converter of ST. Also, the feeder 1 reactive and harmonic current requirements are supplied by the LV converter of ST. Therefore, the MV grid only supplies real power requirements of the city center. The LV converter of ST is rated for the active, reactive, and harmonic support of the load. The dc-dc converter stage of ST is rated for LV ac side active power requirements. Since, the power converters have discrete voltage and current ratings, they will always be slightly overrated. In this paper, it is considered that the MV converter of ST is 20% overrated from the nominal power rating. This allows significant capability to compensate reactive and harmonic power in the MV grid. The parameters for city center is summarized in Table I.

From the power flow diagram and Table I, it is seen that a single ST eliminates need of the CPT from feeder 1 and one SAPF in the city center. Consequently, the overall space requirements will be greatly reduced.

#### V. OPERATION AND CONTROL OF ST

The three stages of ST have different control objectives and are controlled accordingly. Let MV grid currents, ST MV con-

TABLE I  
CITY CENTER PARAMETERS

System configuration	Device power rating and feeder loads
Traditional city center	Transformer T1 = 1.25 MVA, ( $P_1 = 1$ MW, $Q_1 = 0.4$ MVar) Transformer T2 = 1.25 MVA ( $P_2 = 1$ MW, $Q_2 = 0.4$ MVar)
SAPF based city center	Transformer T1 = 1.25 MVA, $P_1 = 1$ MW, $Q_1 = 0.4$ MVar, Transformer T2 = 1.25 MVA, $P_2 = 1$ MW, $Q_2 = 0.4$ MVar, Transformer T3 = 1 MVA, ac-dc converter = 1 MVA
Proposed system (ST based)	ST MV converter = 1.2 MVA ST dc-dc converter = 1 MW ST LV converter = 1.25 MVA ( $P_1 = 1$ MW, $Q_1 = 0.4$ MVar) Transformer T2 = 1.25 MVA, $P_2 = 1$ MW, $Q_2 = 0.4$ MVar

verter currents, feeder II MV side currents, and PCC voltages are denoted by  $i_{mvj}$ ,  $i_{mv1j}$ ,  $i_{mv2j}$  and  $v_{tj}$ , respectively where  $j = a, b, c$  are three phases.

#### A. Control of MV Converter

The ST is operated in such a way that the MV grid currents in the city center are balanced, sinusoidal, and in phase with the respective terminal voltages. Therefore, the reference currents of MV converter of ST consist of two components. Component I of currents include active power demand of feeder 1 LV loads and ST losses, whereas component II of current includes reactive and harmonic currents components of feeder 2 LV loads. Based on instantaneous symmetrical component theory, the reference currents of the MV converter ( $i_{mvj}^*$  where  $j = a, b, c$  are three phases) are computed as follows [13]:

$$i_{mv1j}^* = - \left[ \frac{v_{tj}}{\Delta} (P_1 + P_{loss}) \right] + \left[ i_{mv2j} - \frac{v_{tj}}{\Delta} (P_2) \right] \quad (5)$$

where  $\Delta = (v_{ta})^2 + (v_{tb})^2 + (v_{tc})^2$ . The powers  $P_1$ ,  $P_{loss}$ , and  $P_2$  are average load power demand of feeder I, power losses in the ST, and average load power demand of feeder II, respectively. The power loss  $P_{loss}$  is computed using a proportional integral (PI) controller and it helps in maintaining the MV dc link voltage at a reference voltage.

#### B. Operation of High Frequency dc-dc Converter

This converter steps down the MV dc link voltage to a regulated lower voltage at LV dc link. The power flow balance in the converter circuit is maintained by controlling the phase shift angle ( $\theta$ ) of the pulsed voltages of the two converters linked through the high frequency transformer. The angle  $\theta$  is generated using a PI controller. The reference voltage of the LV dc link is compared with the actual dc link voltage of the ST. The error is passed through the PI controller which results in required phase shift angle  $\theta$  [2].

#### C. Operation of LV dc-ac Converter

The LV converter provides a balanced sinusoidal voltage at a constant frequency at the LV ac distribution system throughout

TABLE II  
PERCENTAGE THDS IN MV GRID CURRENTS WITH RC TYPE NONLINEAR LOAD

System configuration	$i_{ga}$	$i_{gb}$	$i_{gc}$
Without load compensation	11.43	12.18	10.18
With load compensation	1.68	1.60	1.67

the operation. The reference LV ac terminal voltage of the converter is maintained at a constant value of 230 V rms per phase and has a frequency of 50 Hz. These voltages are compared with the actual voltages to generate the control signal [1].

## VI. SIMULATION RESULTS

A switching model of the ST is developed using power system computer aided design (PSCAD) software. Both the feeders have unbalanced reactive and harmonic loads. The Fig. 4(a)-(h) shows PCC voltages, total MV grid currents, MV ST currents, feeder 2 MV currents, LV side ST voltages, LV side ST currents, MV dc link voltage and LV dc link voltage, respectively. Initially, feeder 2 has RL type nonlinear load as well as unbalanced reactive load and at  $t = 0.8$  s the nonlinear load was disconnected. It can be seen from Fig. 4(a) and (b) that the respective phase voltages and currents are in-phase with each other at MV grid and the MV currents are balanced sinusoidal throughout the ST operation. Fig. 4(c) shows the three phase MV side ST currents consisting of real current to support the loads at feeder 1 and the currents needed to compensate the loads connected to the feeder 2. The loads connected to the feeder 2 draw currents as per the requirements and are given in Fig. 4(d). The MV and LV dc link voltages are regulated around its reference values.

The load compensation under a highly distorted RC type nonlinear load is shown in Fig. 5 from time  $t = 0.78$  to 0.8 s. It can be seen that the total MV grid currents are balanced sinusoidal with UPF at the PCC. At time  $t = 0.8$  s, the RC type non linear load is disconnected from feeder 2 and only unbalanced linear loads are connected. In this case, the ST supplies for the unbalance and reactive current compensation of the loads and again makes the grid currents balanced and sinusoidal. No significant variations in dc links of ST are observed.

## VII. POWER HARDWARE IN LOOP (PHIL) SET UP DESCRIPTION AND EXPERIMENTAL RESULTS

The laboratory setup is shown in Fig. 6, where the ST and the grid can be simulated in the RTDS software and can be configured in the control desk via a computer. The control system of the ST is implemented in an external equipment (dSPACE 1006). In order to test these devices under a most realistic condition, the power amplifiers are included in the hardware loop. The measured voltage and current from RTDS will be amplified to the actual values of the grid and sent to the dSPACE through voltage/current sensors as well as other power interfaces. In this case, the power converters that represent different ST stages can be controlled and subjected

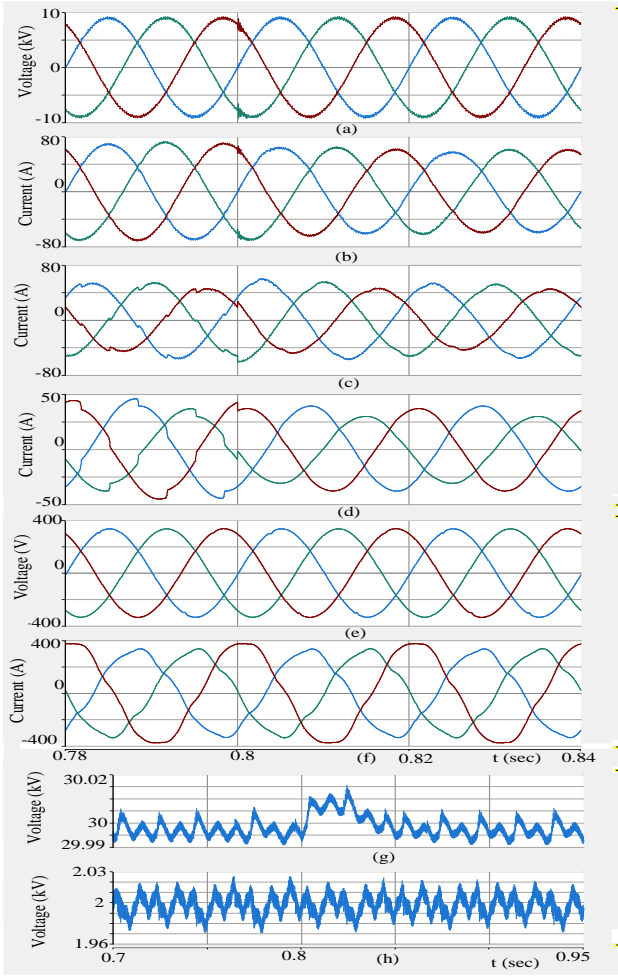


Fig. 4. Compensating waveforms when RL type nonlinear load is removed at  $t = 0.8$  s from feeder 2. (a) PCC voltages. (b) Total MV grid currents. (c) MV ST currents. (d) Feeder 2 MV currents. (e) LV side ST voltages. (f) LV side ST currents. (g) MV dc link voltage. (h) LV dc link voltage.

under an actual grid condition. The methodology and laboratory setup can be generalized for any ST-fed grid.

The experiments are done with the reduced scale set-up. The schematic of set-up is shown in Fig. 6(b). A voltage of 311 V, 50 Hz is realized by the power source. The ST is realized by an ac/dc converter (4 kW power rated operating at 10 kHz switching frequency) with resistive load at its dc link. The ST converter is connected to the grid through an LC filter whose inductance is 5.6 mH, the capacitance is 5  $\mu$ F in series with a resistance of 1.2  $\Omega$ . In feeder 2, three phase diode bridge rectifier based RC type nonlinear load is connected. For this system, the experimental waveforms are shown in Fig. 7. The total grid currents, as shown in Fig. 7(a), are distorted due to the harmonic loads in feeder 2. The ST load compensation feature is not activated and it takes balanced sinusoidal currents for support of its load as shown in Fig. 7(b). In contrast, the grid performances are improved by means of the ST as shown in Fig. 7(c) where the total grid

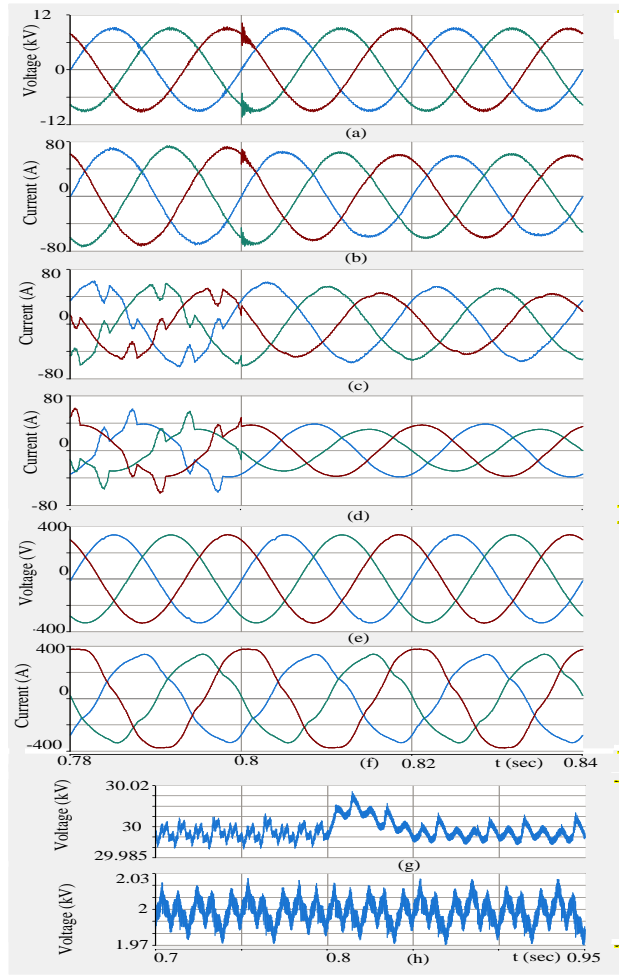


Fig. 5. Compensating waveforms when RC type nonlinear load is removed at  $t = 0.8$  s from feeder 2. (a) PCC voltages. (b) Total MV grid currents. (c) MV ST currents. (d) Feeder 2 MV currents. (e) LV side ST voltages. (f) LV side ST currents. (g) MV dc link voltage. (h) LV dc link voltage.

currents have become balanced and sinusoidal. The harmonic currents of feeder 2 are supplied by the ST, while it supports its own loads, as shown in Fig. 7(d). The frequency spectrum shown in the waveforms shows the improvement in THDs of the grid currents.

## VIII. CONCLUSIONS

This paper has investigated the load compensation features of an ST in the two-feeder city center. A detailed analysis of the sizing and compensation capability of the ST has been carried out. Through the developed PSCAD based switching model and experimental prototype, the compensation features of the ST are verified. It is shown that the ST compensates for the unbalance, reactive, and harmonic components of the loads connected at the feeder supplied by the CPT, in addition to supplying their own loads. This scheme eliminates the requirement of power quality improvement devices like SAPF, power factor correcting capacitors, etc., connected at

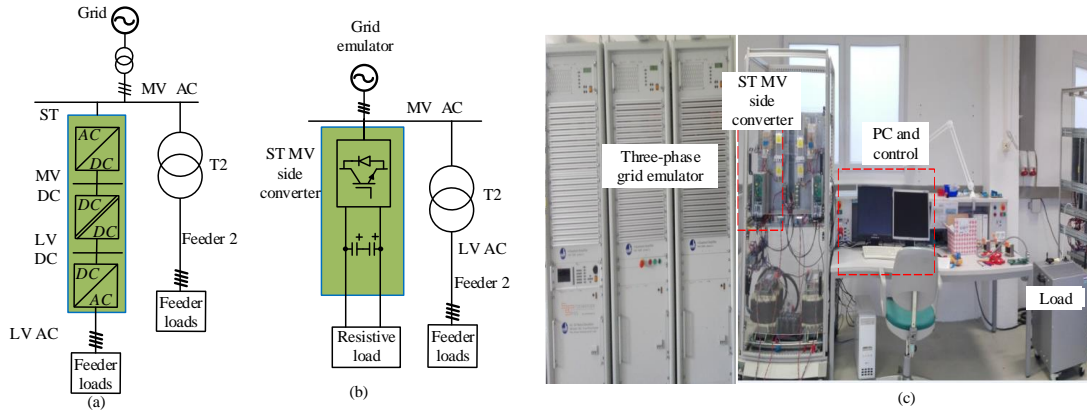


Fig. 6. (a) ST based two feeder city center. (b) Laboratory setup schematic. (c) Laboratory setup photograph.

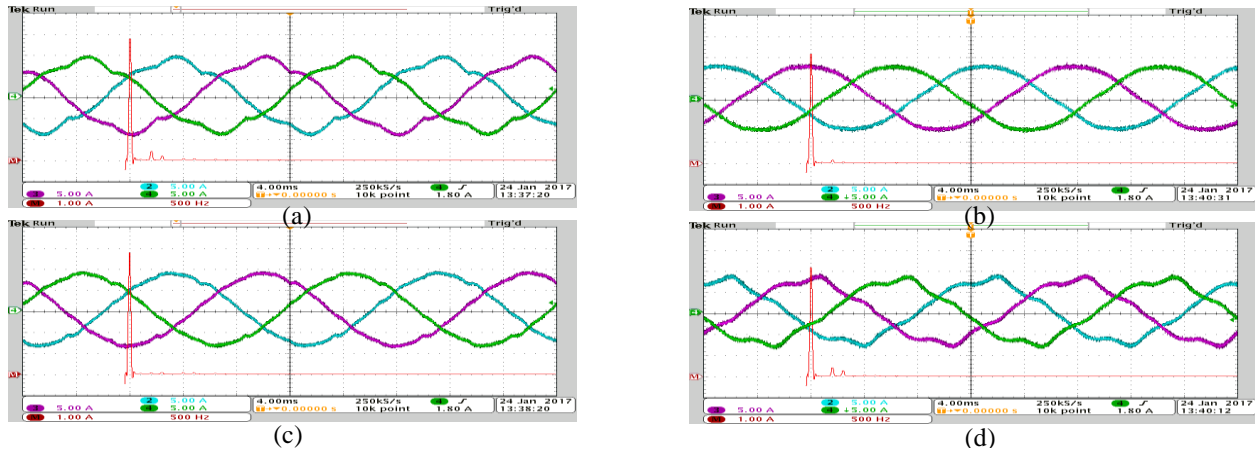


Fig. 7. Grid performances. (a) Total grid currents when ST load compensation feature is not activated. (b) ST currents when its load compensation feature is not activated. (c) Total grid currents after activating load compensation features of ST. (d) ST currents after activation of load compensation features.

the second feeder. These additional features in the city-center make the application of ST attractive.

## IX. ACKNOWLEDGMENT

This work is supported by the Alexander von Humboldt Foundation, Germany and the European Research Council under the European Unions Seventh Framework Programme (FP/2007-2013) / ERC Grant Agreement no. [616344].

## REFERENCES

- [1] R. Teodorescu, M. Liserre, and P. Rodriguez, *Grid converters for photovoltaic and wind power systems*. John Wiley & Sons, 2011, vol. 29.
- [2] M. Liserre, G. Buticchi, M. Andresen, G. D. Carne, L. F. Costa, and Z. X. Zou, "The smart transformer: Impact on the electric grid and technology challenges," *IEEE Ind. Electron. Mag.*, vol. 10, no. 2, pp. 46–58, June 2016.
- [3] S. Bhattacharya, "Transforming the transformer," *IEEE Spectrum*, vol. 54, no. 7, pp. 38–43, July 2017.
- [4] X. She, A. Huang, and R. Burgos, "Review of solid-state transformer technologies and their application in power distribution systems," *IEEE Trans. Emerg. Sel. Topics Power Electron.*, vol. 1, no. 3, pp. 186–198, Sep. 2013.
- [5] Z. X. Zou, M. Liserre, Z. Wang, M. Cheng, and S. Fan, "Resonance damping in a smart transformer-based microgrid," in *41st Annual Conference of the IEEE Industrial Electronics Society, IECON 2015*, Nov 2015, pp. 956–964.
- [6] G. D. Carne, G. Buticchi, M. Liserre, and C. Vournas, "Load control using sensitivity identification by means of smart transformer," *IEEE Trans. Smart Grid*, vol. PP, no. 99, pp. 1–1, 2016.
- [7] C. Kumar and M. Liserre, "Operation and control of smart transformer for improving performance of medium voltage power distribution system," in *6th IEEE International Symposium on Power Electronics for Distributed Generation Systems (PEDG)*, June 2015, pp. 1–6.
- [8] Z. Shen, Z. Wang, and M. Baran, "Optimal volt/var control strategy for distribution system with multiple voltage regulating devices," in *IEEE PES Transmission and Distribution Conference and Exposition (TD)*, 2012, May 2012, pp. 1–7.
- [9] D. Shah and M. Crow, "Online volt-var control for distribution systems with solid state transformers," *IEEE Trans. Power Del.*, vol. PP, no. 99, pp. 1–1, 2015.
- [10] C. Kumar and M. Liserre, "A new prospective of smart transformer application: Dual microgrid (dmg) operation," in *41st Annual Conference of the IEEE Industrial Electronics Society; IECON 2015*, Nov 2015, pp. 004482–004487.
- [11] S. B. Karanki, N. Gedda, M. K. Mishra, and B. K. Kumar, "A dstatcom topology with reduced dc-link voltage rating for load compensation with nonstiff source," *IEEE Trans. Power Electron.*, vol. 27, no. 3, pp. 1201–1211, March 2012.
- [12] A. Bhattacharya, C. Chakraborty, and S. Bhattacharya, "Parallel-connected shunt hybrid active power filters operating at different switching frequencies for improved performance," *IEEE Trans. Ind. Electron.*, vol. 59, no. 11, pp. 4007–4019, Nov 2012.
- [13] A. Ghosh and G. F. Ledwich, *Power quality enhancement using custom power devices*. Kluwer academic publishers, 2002.